Tetraodon nigroviridis as a nonlethal model of infectious spleen and kidney necrosis virus (ISKNV) infection

Xiaopeng Xu [a],[1], Lichao Huang [a],[1], Shaoping Weng [a], Jing Wang [a], Ting Lin [a], Junliang Tang [a], Zhongsheng Li [a], Qingxia Lu [a], Qiong Xia [a], Xiaoqiang Yu [b], Jianguo He [a],*

[a] State Key Laboratory of Biocontrol, School of Life Sciences, Sun Yat-sen (Zhongshan) University, Guangzhou, PR China
[b] Division of Cell Biology and Biophysics, School of Biological Science, University of Missouri-Kansas City, Kansas City, KS, USA

ARTICLE INFO

ABSTRACT

Infectious spleen and kidney necrosis virus (ISKNV) is the type species of the genus Megalocytivirus, family Iridoviridae. We have previously established a high mortality ISKNV infection model of zebrafish (Danio rerio). In this study, a nonlethal Tetraodon nigroviridis model of ISKNV infection was established. ISKNV infection did not cause lethal disease in Tetraodon but could infect almost all the organs of this species. Electron microscopy showed ISKNV particles were present in infected tissues. Immunofluorescence and quantitative real-time PCR analysis showed that nearly all the virions and infected cells were cleared at 14 d postinfection. The expression profiles of interferon-γ and tumor necrosis factor-α gene in response to ISKNV infection were significantly different in Tetraodon and zebrafish. The establishment of the nonlethal Tetraodon model of ISKNV infection can offer a valuable tool complementary to the zebrafish infection model for studying megalocytivirus disease, fish immune systems, and viral tropism.

© 2010 Elsevier Inc. All rights reserved.

Introduction

Iridoviruses are a group of icosahedral cytoplasmic DNA viruses with circularly permuted and terminally redundant DNA genomes that can infect invertebrates and poikilothermic vertebrates, including insects, fish, amphibians, and reptiles (Williams, 1996; Darai et al., 1983, 1985; Delius et al., 1984; Tidona and Darai, 1997). The family Iridoviridae is divided into five genera: Iridovirus, Chloriridovirus, Ranavirus, Lymphocystivirus, and Megalocytivirus (Chinchar et al., 2005). Megalocytivirus infection is characterized by marked hypertrophy of infected cells and is one of the most harmful viruses to cultured fish (Chinchar et al., 2005; Inouye et al., 1992; Jung and Oh, 2000). Infectious spleen and kidney necrosis virus (ISKNV), the causative agent of a disease causing high mortality in mandarin fish, Siniperca chuatsi, is regarded as the type species of the Megalocytivirus genus (Chinchar et al., 2005). ISKNV-like viruses can also infect large-mouth bass, Micropterus salmoides, Murray cod, Maccullochella peelii peelii, and more than 60 other species of marine and freshwater fish (Go et al., 2006; Wang et al., 2007; Jeong et al., 2008). Cell hypertrophy in spleen, kidney, cranial connective tissues, and endocardia is the typical sign of ISKNV infection in mandarin fish (He et al., 2000, 2002). The genome of ISKNV (GenBank accession no. AF371960) is highly methylated and was sequenced in 2001 (He et

al., 2001). We have previously reported a zebrafish (Danio rerio) model of ISKNV infection, which is the first established DNA virus-zebrafish infection model (Xu et al., 2008). ISKNV infection of zebrafish results in high mortality and causes similar symptoms, such as organ hemorrhage and cell hypertrophy, to those of mandarin fish. Both the zebrafish and ISKNV genomes have been sequenced; thus, the ISKNV-infected zebrafish model is likely to prove very useful in the study of the interactions between ISKNV and its host.

The green-spotted pufferfish, Tetraodon nigroviridis, has the smallest known vertebrate genome (~350 Mb) (Roest Crollius et al., 2000b; Volff et al., 2003). The genome of Tetraodon was sequenced in 2004 (Jaillon et al., 2004). The genome catalogue and gene structures of Tetraodon are very similar to those of humans and zebrafish. With short introns and small intergenic regions, the Tetraodon genome is highly compact, being eight times smaller than that of humans and four times smaller than that of zebrafish (Volff, 2005; Roest Crollius et al., 2000a). These advantages make Tetraodon ideal for genomic studies, which may help in the annotation and functional studies of genes in other species (Lutfalla et al., 2003). Furthermore, Tetraodon is potentially a novel model fish, in addition to zebrafish, for further use in various research areas, such as developmental biology, immunology, physiology, biochemistry, genetics, and evolutionary biology (Bui et al., 2010; Clelland et al., 2010; Sepulcre et al., 2009).

In this study, we established an ISKNV-Tetraodon infection model. ISKNV can successfully infect Tetraodon cells. This is the first report of virus infection in Tetraodon. The infected cells were present in almost all organs, especially in the spleen and kidney. However, ISKNV infection

---

* Corresponding author. School of Life Sciences, Sun Yat-sen (Zhongshan) University, Guangzhou, 510275, P.R China. Fax: +86 20 84113229.
E-mail address: lsshjg@mail.sysu.edu.cn (J. He).
[1] These authors contributed equally to this work.

did not cause death in *Tetraodon*, and nearly all the ISKNV-infected cells were cleared at 14 d postinfection (dpi), suggesting that *Tetraodon* can resist the lethality of ISKNV infection. The expression of interferon-γ (IFN-γ) and tumor necrosis factor-α (TNF-α) was significantly different in the ISKNV-infected *Tetraodon* and zebrafish, which may help to explain why *Tetraodon* can survive ISKNV infection while zebrafish cannot. Complementary to zebrafish, the *Tetraodon* model of ISKNV infection may serve as an important platform for the studies of megalocytivirus disease, fish immune systems, and viral tropism.

Result

Clinical signs

We found that *Tetraodon* was hard to be infected by challenge using immersion method. The experiments to challenge *Tetraodon* using intraperitoneal injection method have been repeated many times using different viral doses. No *Tetraodon* died after challenging with all these low or high doses. We found that challenging with low dose of virus, the cell infection rates in *Tetraodon* tissues were also low (data not shown). In order to obtain a high tissue infection rate, the viral dose was normalized to 25 μL/g body weight of ISKNV at 4×10^{11} genome equivalents (GE)/mL. Following inoculation with this dose, a concentration that was approximately double that used in the establishment of zebrafish infection (Xu et al., 2008), no *Tetraodon* died from ISKNV infection in the 6 weeks period postinoculation, whereas all the infected zebrafish were dead by 9 dpi (Fig. 1). Compared with the control fish, the spleen and intestine of the challenged *Tetraodon* showed obvious signs of enlargement at 8 dpi, and return to normal after 14 dpi.

Histopathology and electron microscopy

Histopathology studies by comparing the spleens and kidneys of the control and ISKNV-infected fish at 8 dpi revealed that the spleens of control fish contained normal white and red pulp regions and brown granules present in the areas involved in erythrocyte phagocytosis (Fig. 2A). In contrast, the spleens of ISKNV-infected *Tetraodon* showed signs of hyperemia and reduction of the areas containing brown granules (Fig. 2B). In the kidneys of infected fish (Fig. 2C), the glomeruli showed slight shrinkage, and the areas between renal tubules and glomeruli appeared less tightly arranged compared to those of control fish (Fig. 2D). Unlike in mandarin fish (He et al., 2000, 2002), only a few hypertrophic cells can be stained by hematoxylin in the spleens and
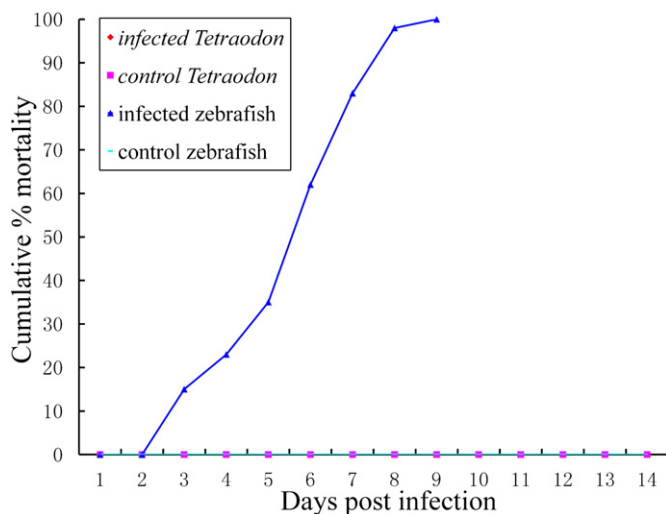

Fig. 1. The cumulative mortalities of *Tetraodon* and zebrafish challenged with 25 μL/g body weight of purified ISKNV at 4×10^{11} GE/mL. No *Tetraodon* died from infection, whereas all the infected zebrafish were dead by 9 dpi.

kidneys of ISKNV-infected *Tetraodon* (Figs. 2B and D, blue arrows). Other organs showed no significant signs of pathological changes. Histological changes in infected *Tetraodon* tissues were milder than those observed in mandarin fish and zebrafish (He et al., 2000, 2002; Xu et al., 2008).

The spleen sections of ISKNV-infected *Tetraodon* at 8 dpi were examined by electron microscopy (EM). Discrete areas containing abundant virus particles were observed in infected cells (Fig. 2E). The ISKNV particles were approximately 150–200 nm, the same size as described in the infected mandarin fish cells (He et al., 2000, 2002). The mature virions had cores and were located along side immature virus particles that appeared to be undergoing assembly (Fig. 2F).

Tissues distribution of the infected cells

The paraformaldehyde-fixed, paraffin-embedded sections of organs from *Tetraodon* at 8 dpi were stained by immunohistochemistry using the polyclonal mouse antisera against viral protein VP23R, as previously described (Xu et al., 2008). Like in zebrafish, the ISKNV-infected cells were present in almost all organs of the infected *Tetraodon* (Fig. 3) with an exception of the skin tissues where the infected cells were difficult to be found (Fig. 3L). Interestingly, the infected cells showed different locations in the kidney at 8 and 12 dpi. At 8 dpi, the infected cells existed in the gap regions between renal tubules and inside some of the renal glomeruli but not in the epithelia region of renal tubules (Fig. 3B). At 12 dpi, more infected cells were found inside the renal glomeruli than in the gap regions, and the infected cells were also found inside the lumen of the renal tubules (Fig. 3C).

ISKNV infection kinetics in Tetraodon tissues

To study features of ISKNV infection and replication in *Tetraodon* at different stages of infection, double-stain immunofluorescence analysis was performed with VP23R protein visualized in green fluorescence under stimulation of 488 nm light and major capsid protein (MCP) visualized in red fluorescence under 633 nm light stimulation. Infected spleens were sampled from 3 to 14 dpi (Fig. 4A). The number of the infected cells increased from 3 dpi to 8 dpi. After peaking at 8 dpi, the number of the infected cells began to decrease until almost all the infected cells were cleared at 14 dpi. The red fluorescence signals representing MCP antigen began to appear at 6 dpi, and the release of virus particles from infected cells (Fig. 4A, white arrows) was observed at 8 dpi, peaked at 10 dpi, and nearly all the MCP signals disappeared after 12 dpi. As controls, the infected spleens were detected using mock-immunized sera and the mock-infected spleens were detected using anti-VP23R and anti-MCP specific antibodies. No fluorescent signals were observed (data not shown). As a comparison, immunofluorescence analyses demonstrated that the number of the infection cells in zebrafish spleens also reached a peak at 8 dpi (Fig. 4A). All the infected zebrafish were dead by 9 dpi and did not undergo a recovery period. MCP antigen signals were less abundant in zebrafish spleens than in *Tetraodon*.

Consistent with the results of immunofluorescence analyses, the quantitative analysis of ISKNV GE using quantitative real-time PCR revealed variations in the quantities of virus DNA present in the infected spleens of *Tetraodon* and zebrafish at various time points postinfection (Fig. 4B). In *Tetraodon* spleens at 1–3 dpi, the quantity of viral DNA was extremely low ($<8.55 \times 10^5$ GE/μg DNA). Viral DNA subsequently increased in concentration up to a maximum of 3.17×10^7 GE/μg DNA at 10 dpi. The quantity of viral DNA then decreased rapidly to 3.94×10^5 GE/μg DNA at 14 dpi (Fig. 4B). In zebrafish spleens, the concentrations of ISKNV DNA also showed an increase during infection and reached a maximum of 7.52×10^6 GE/μg DNA at 8 dpi.

Transcription of the VP23R and MCP genes of ISKNV was also examined in infected spleen cells at 0.5, 1, 1.5, 2, 3, 4, 5, 6, 8, 10, 12, and 14 dpi by quantitative real-time reverse transcription–PCR (RT–PCR) (Fig. 4C). Periodic expression of the VP23R gene was detected with
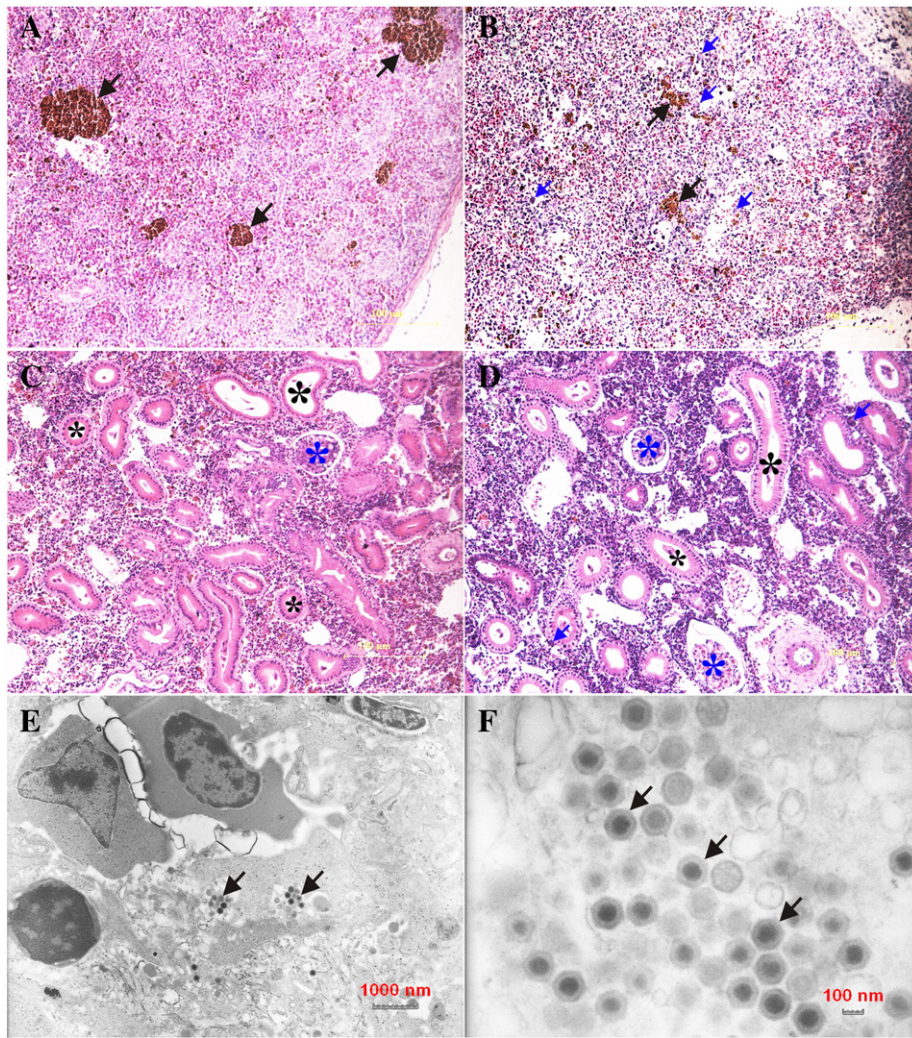
Fig. 2. Histopathology (magnification, ×400) and EM analyses of *Tetraodon* tissues at 8 dpi. Histopathology showed that the spleens of healthy control fish (A) contained normal white and red pulp regions and the brown granules collected areas (black arrows). Spleen tissues of ISKNV-infected *Tetraodon* (B) showed signs of hyperemia and reduction of the brown granules collected areas (black arrows). In the kidney of control fish (C), black asterisks indicate renal tubules and blue asterisks indicate the glomeruli. In the kidney of the infected fish (D), the glomeruli showed slight shrinkage and the areas between the renal tubules and glomeruli appeared less tightly arranged. In (B) and (D), the hypertrophic cells stained by Hematoxylin were marked with blue arrows. EM analysis showed that virions scattered within the spleen tissues (E) (magnification, ×5200) and gathered inside infected cells (F, black arrows) (magnification, ×28,500).

peaks at 2 and 6 dpi, but the expression level of the second peak at 6 dpi was only 29.5% of that of the first peak at 2 dpi. MCP transcription was barely detectable before 3 dpi. At 3–4 dpi, MCP transcription increased sharply and reached a peak value at 5 dpi and then declined to the basal level after 10 dpi.

Expression profile analysis of immune-related genes

Expression of antiviral immune-related genes in the ISKNV-infected zebrafish and *Tetraodon* was determined by quantitative real-time RT–PCR (Fig. 5). Following inoculation, the expression of *Tetraodon* type I IFN gene was upregulated by 9–10 folds, with two peaks at 16 h postinfection (hpi) and 4 dpi. The expression of zebrafish type I IFN gene increased 7–14 folds, with three peaks at 4 and 24 hpi, and 3 dpi. The magnitude of the changes in IFN-α expression in the two fishes was similar, although the temporal patterns were slightly different. Compared with the controls, the expression of zebrafish IFN-γ gene showed no apparent change, whereas *Tetraodon* IFN-γ transcription was significantly upregulated periodically, with the first peak of 18-fold increase at 16 hpi and the second peak of 52- to 54-fold increase at 3 to 4 dpi. The TNF-α expression in *Tetraodon* exhibited a 3-fold increase at 4 hpi and then returned to the basal level at 24 hpi where it remained

unchanged. In contrast, the expression of zebrafish TNF-α changed markedly after infection, showing a sharp increase at 24 hpi which was maintained at 67- to 43-fold levels of up-regulation up to 2 dpi, followed by a sharp decline at 3 dpi.

Discussion

Virus infection has not yet been reported in *Tetraodon*. The establishment of a nonlethal *Tetraodon* model of ISKNV infection filled this gap. As an ideal genomic study model organism, *Tetraodon* has such a compact and sequenced genome that makes it easy to identify the immune-related genes and characterize their modulation roles in the process of antiviral immunity. ISKNV can cause high mortality in zebrafish but does not cause death in *Tetraodon*, so these two infection models may be complementary in the study of ISKNV infectious disease, greatly facilitating studies of the fish immune system, ISKNV gene function, lethality mechanisms of megalocytiviruses, and virus–host interactions.

Tetraodon survived ISKNV infection despite being challenged with a high titer of virus particles. The pathological changes in infected *Tetraodon* tissues were milder than those of mandarin fish and zebrafish, although cell infection rates in the *Tetraodon* tissues were similar to
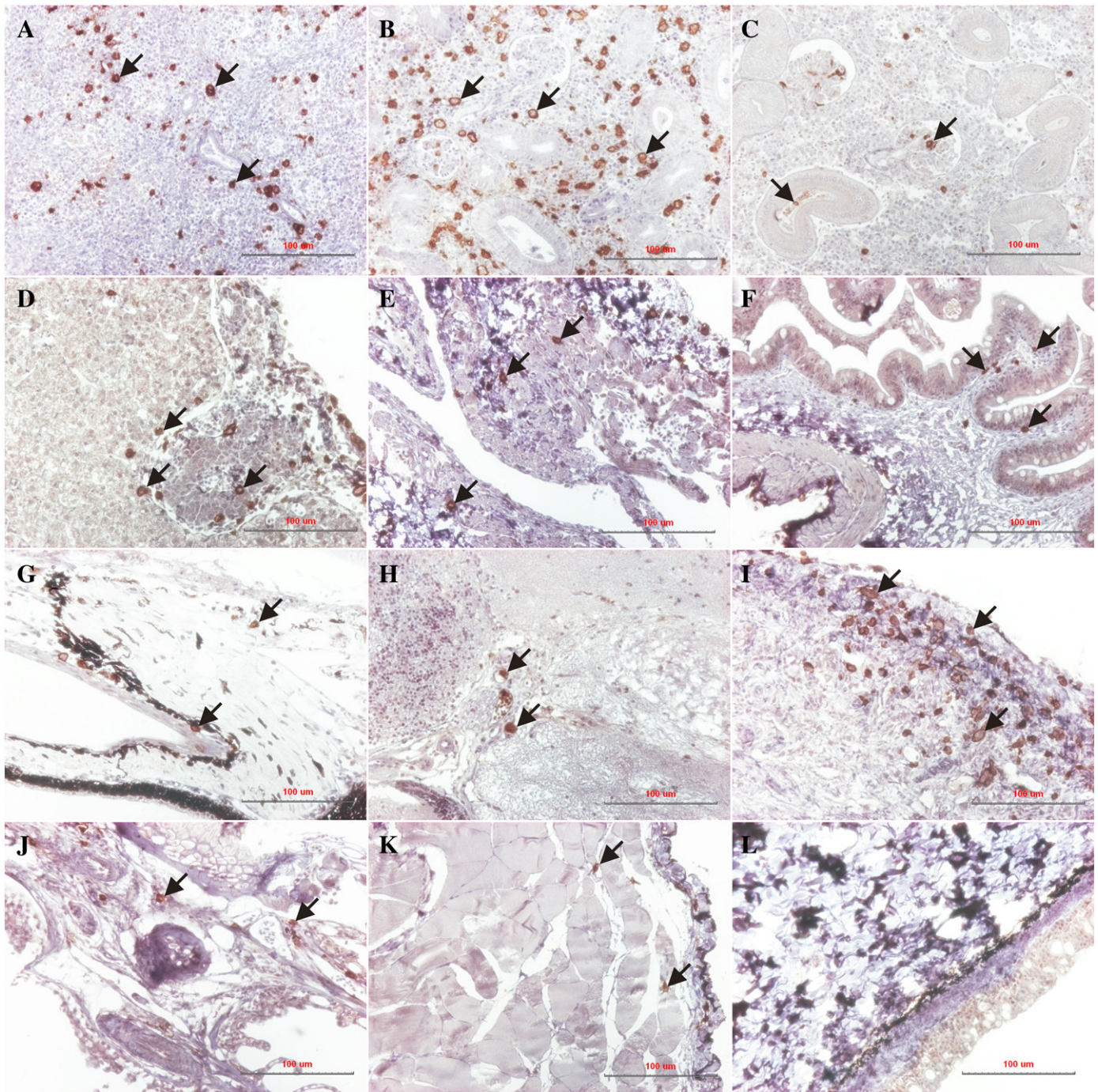
Fig. 3. Immunohistochemical examination of *Tetraodon* infected with ISKNV by i.p. injection at 8 dpi (magnification, ×400). The *Tetraodon* sections were incubated with polyclonal mouse antisera against viral protein VP23R and developed using diaminobenzidine (DAB) mixture. The ISKNV-infected cells were specifically stained brown (black arrows). (A) spleen, (B) kidney (at 8 dpi), (C) kidney (at 12 dpi), (D) liver, (E) heart, (F) digestive tract, (G) eyes, (H) brain, (I) sex gland, (J) gill, (K) muscle, and (L) skin.

those observed in mandarin fish and zebrafish hosts (He et al., 2000, 2002; Xu et al., 2008). The prevalence of infection in cells of *Tetraodon* tissues reached a peak at 8 dpi, when the tissues exhibited obvious pathological changes, and then decreased rapidly to a very low level at 14 dpi, when the clinical signs of infection also disappeared. This indicates that *Tetraodon* was able to clear ISKNV infection. Changes in the quantities of ISKNV genomic DNA in spleen tissues during the infection also support this conclusion. ISKNV genomic DNA concentration peaked at 10 dpi and then almost disappeared at 14 dpi, suggesting that the infection had been cleared.

It has been speculated that ISKNV can spread through the host circulation system (Xu et al., 2008). ISKNV-infected hypertrophic cells were present in almost all zebrafish organs, including spleen, kidneys, liver, gills, esophagus, gut, muscles, and eyes (Xu et al., 2008). In *Tetraodon*, we also observed ISKNV infecting almost all organs, suggesting that ISKNV-susceptible cells may be common in *Tetraodon* and zebrafish. The infected cells in the kidney of *Tetraodon* were mainly present in renal glomeruli at 12 dpi when most infected cells had disappeared in the gap areas between renal tubules. Renal glomeruli are blood capillary-rich areas; therefore, this observation supports the idea that ISKNV spreads through the circulation system. The infected cells localized in the renal tubule lumens may be derived from renal glomeruli.

ISKNV infection of *Tetraodon* is a nonlethal model and of zebrafish is a high-mortality model; therefore, the clinical signs and pathological
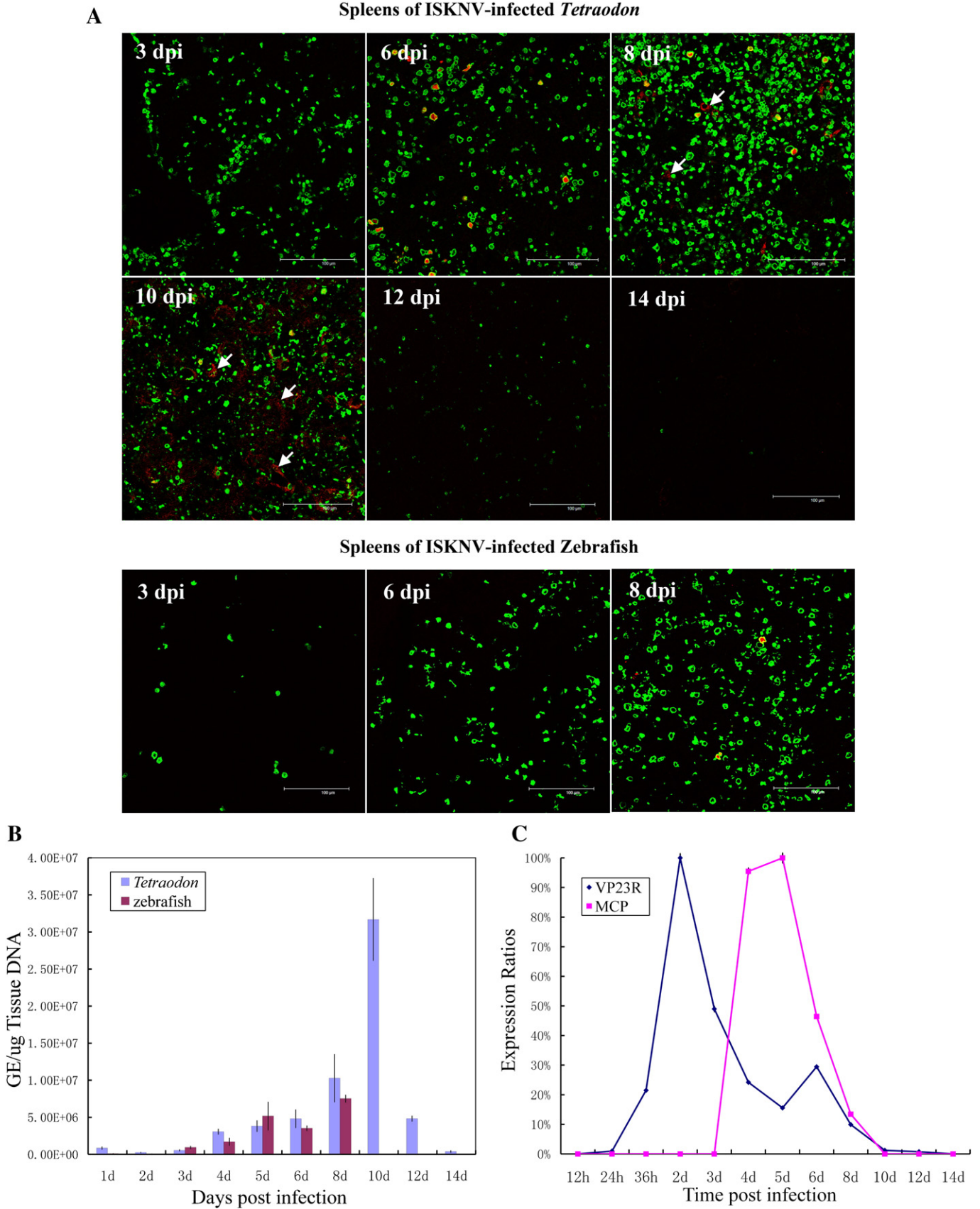
Fig. 4. (A) Double-stain immunofluorescence analysis of spleens from ISKNV-infected *Tetraodon* and zebrafish. Infected cells were labeled with Alexa Fluor 488 (Invitrogen, USA) for VP23R (green fluorenscence) and the ISKNV particles were labeled with Alexa Fluor 633 (Invitrogen, USA) for MCP (red fluorenscence). White arrows indicate the released virions. (B) Quantitative real-time PCR analysis of ISKNV GE in the spleen tissues of infected *Tetraodon* and zebrafish at various time points postinfection. (C) Quantitative real-time RT–PCR analysis of ISKNV VP23R and MCP mRNA expression in ISKNV-infected *Tetraodon* at 12, 24, and 36 hpi and 2, 3, 4, 5, 6, 8, 10, 12 and 14 dpi.
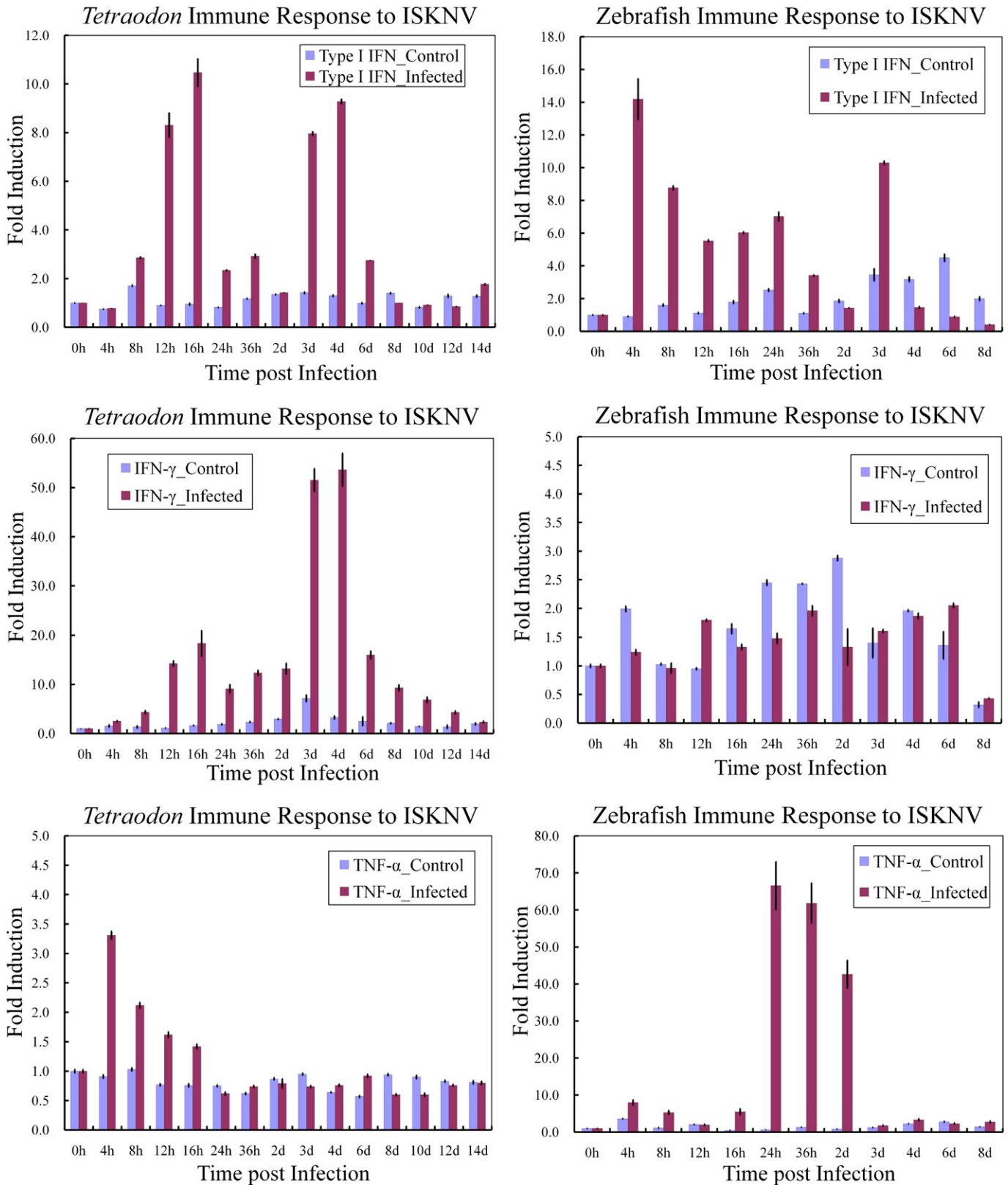
Fig. 5. Comparison of the type I IFN, IFN-γ, and TNF-α gene expression profiles in response to ISKNV infection in *Tetraodon* and zebrafish.

changes in tissues and the behavior of virus inside the cells of the two species differ significantly. In zebrafish, MCP synthesis, viral particle assembly, and release were blocked to a certain extent due to still unknown mechanisms (Xu et al., 2008). MCP antigen signals were more abundant in *Tetraodon* tissues than in zebrafish, and the released virions

were readily detected in *Tetraodon* at 10 dpi, suggesting that *Tetraodon* cells may be more suitable for replication and maturation of ISKNV particles than zebrafish cells. This is probably because *Tetraodon* is phylogenetically closer to mandarin fish than zebrafish. However, *Tetraodon* experienced no mortality following ISKNV infection, whereas

mortality of the infected zebrafish was high (Xu et al., 2008), indicating that replication and release of virions are unlikely to be main reasons for host death. Infection rates of *Tetraodon* cells were much higher and peaked at 8 dpi, when the infected organs showed slight signs of disease. However, no death of the host occurred, suggesting that cell infection rate is also unlikely to be directly related to host mortality. Similarly, for the neurovirulent Sindbis virus (SINV), viral replication and infection rate also have little to do with host death. In this case, the failure of the host immune response, but not the proliferation of the SINV infection itself, is the cause of host death (Rowell and Griffin, 2002). Further studies are needed to elucidate the mechanisms that modulate the lethality of ISKNV infection.

The antiviral immune responses against ISKNV of zebrafish and *Tetraodon* were subjected to preliminary comparison by quantitative real-time RT–PCR. The expression profiles of three antiviral immune-related genes, including types I and II IFN and TNF-α, in response to ISKNV infection were examined and compared. The response profiles of type I IFN genes, which showed periodic up-regulation that may relate to the virus replication cycle, were similar in both hosts, whereas those of type II IFN (IFN-γ) showed a significant difference. ISKNV induced IFN-γ expression at a much higher level in *Tetraodon* than in zebrafish. IFN-γ has antiviral activity and is also an immunomodulatory protein that can activate Th1 cells to initiate cellular immunity (Novelli and Casanova, 2004; Dardalhon et al., 2008; Templeton and Perlman, 2008). It has been reported that cellar immunity plays a crucial role in protecting fish against red seabream iridovirus (RSIV), another important member of the *Megalocytivirus* genus (Caipang et al., 2006). Thus, dramatically upregulated expression of IFN-γ following infection can probably explain why infected cells in *Tetraodon* can be completely cleared without causing serious adverse effects on the host.

ISKNV infection can induce much higher transcription levels of the TNF-α gene in zebrafish than in *Tetraodon*. It is well known that TNF-α plays a critical role in proinflammation and immunoregulation and can partially mediate cellular immunity against infections of bacteria, parasites, and viruses (Bradley, 2008; Cawthorn and Sethi, 2008; Wilhelm et al., 2005). However, overexpression of TNF-α has a toxic effect on normal tissues and can cause severe pathological effects (Katagiri et al., 2008; Kudo et al., 2009; Song et al., 2008). In dengue virus-infected patients, the elevation of TNF-α expression results in endothelial cell apoptosis, vascular leakage, and hemorrhage (Atrasheuskaya et al., 2003; Chen et al., 2007; Martina et al., 2009). Interestingly, organ hemorrhage is one of the typical signs of megalocytivirus infection (Chinchar et al., 2005). A possible explanation for this is that overexpression of TNF-α in zebrafish and suppression of it in *Tetraodon* resulted in more severe tissue damage in zebrafish than in *Tetraodon*. This may also be related to the high mortalities of infected zebrafish. This hypothesis requires further study. Moreover, the expression profiles of TNF-α in infected zebrafish showed sharp changes from 16 to 48 hpi. Further studies are also required to determine if the 32-h period of high expression of TNF-α causes adverse effects on the infected host.

The difference in the expression of the IFN-γ and TNF-α in the two fish may help to explain why *Tetraodon* can survive ISKNV infection while zebrafish cannot. These results support the idea that cytokines play an important role in viral tropism (McFadden et al., 2009). Then, the ISKNV infection models of *Tetraodon* and zebrafish may also provide a useful platform for studies of viral tropism. Moreover, further studies on the comparison of other immune-related genes and signal pathways in the two fish should be performed to identify possible prevention and cure measures for megalocytivirus infection.

Materials and methods

Fish and virus

Wild-type *Tetraodon*, weighing about 10 g each, were bought from a pet market in Guangzhou, China. Fish were maintained in clean water containing 1.5‰ sea salt in a 40-L tank with recirculating and filtering units and a 12-h light/12-h dark cycle at 28 °C and fed with chironomid larvae. Each tank contains 30 fish. Wild-type zebrafish were maintained as previously described (Xu et al., 2008). Fish were maintained more than 10 days before the experiment. Before infection experiments, fish were confirmed free of ISKNV infection by PCR as previously described (Deng et al., 2000; Wang et al., 2007). Briefly, 10% cultured fish were randomly sacrificed and the spleens were sampled. DNA from each sample was extracted as a template. The first-step PCR was performed using ISKNV MCP-specific primers (mF1, 5′-AGACCCACTTGTACGGCG-3′; mR1, 5′-CCCATGTCCAACGTATAGC-3′). Nested PCR was performed using primer mF2 (5′-CGTGAGACCGTGCGTAGT-3′) and mR2 (5′-AGGGTGACGGTCGA-TATG -3′). Each sample was detected in triplicates to confirm the result.

ISKNV was purified from diseased mandarin fish identified in our laboratory (He et al., 2002) and propagated in a cultured mandarin fish fry cell line (MFF-1) (Dong et al., 2008). The supernatants of ISKNV infected cells at 6 dpi were collected and ISKNV particles were purified by sucrose gradient centrifugation. The residual sucrose was eliminated by ultrafiltration using a 100-kDa cutoff membrane (Millipore, USA). Purified ISKNV particles were quantitated by quantitative real-time PCR as previously described (Xu et al., 2008) and diluted in phosphate-buffered saline (PBS; pH 7.4) to 4×10^{11} ISKNV GE/mL. The titer of the virus in diluted PBS was determined in MFF-1 cells as previously described (Dong et al., 2008) as $10^{7.2}$ 50% tissue culture infective dose ($TCID_{50}$)/0.1 mL.

To determine the mortality of *Tetraodon* caused by ISKNV infection, adult *Tetraodon* were injected intraperitoneally (i.p.) with 25 μl/g body weight of the purified ISKNV particles (infection group, $n = 60$) or PBS (control group, $n = 60$) supplemented with 50 IU/mL penicillin and 50 μg/mL streptomycin. As comparisons, 3-month-old zebrafish weighing about 1 g were challenged with 25 μL of the purified ISKNV (infection group, $n = 60$) or PBS (control group, $n = 60$) in the same way.

Histology analysis

Spleens and kidneys of 20 ISKNV-infected *Tetraodon* at 8 dpi were sampled for histology and placed in 10 mL of buffered 10% formalin. The samples were dehydrated by passage through a gradient of ethanol solutions, embedded in paraffin, and cut into 4-μm-thick sections. The sections were stained with hematoxylin and eosin for microscopic examination.

EM analysis

Spleens of 20 ISKNV-infected *Tetraodon* at 8 dpi were fixed in 2.5% glutaraldehyde in 0.1 M phosphate buffer (pH 7.4). The specimens were rinsed with 0.1 M phosphate buffer four times and postfixed in 0.1 M phosphate buffer containing 2.0% osmium tetroxide for 1 h at 4 °C and embedded in Epon's 812 following dehydration. Ultrathin sections were cut, stained with uranyl acetate and lead citrate, and examined on a Philips CM10 EM for the presence of virus particles in hypertrophic cells.

Immunohistochemistry and immunofluorescence analyses

Spleens of ISKNV-infected *Tetraodon* at 3, 6, 8, 10, 12, and 14 dpi, and zebrafish at 3, 6, and 8 dpi were sampled, fixed with 4% paraformalde-hyde, paraffin-embedded, and sectioned. Immunohistochemistry and immunofluorescence analyses of the VP23R and MCP of ISKNV were performed as previously described (Xu et al., 2008). As controls, the ISKNV-infected spleens of *Tetraodon* at 8 dpi were detected using sera from PBS-mock immunized mice and rabbits, and the PBS mock-infected spleens were also detected using mice anti-VP23R polyclonal antibodies and rabbit anti-MCP polyclonal antibodies.

Table 1
Analyzed genes and their specific primers.

Gene name	Species name	Primer sequence (5′–3′)	GenBank accession no.
VP23R	ISKNV	F: 5′-GCCACGCCACCACCTTCTATAAC-3′	AF371960-ORF023
		R: 5′- TGTCGCTTGCCCAAACAATCTTC-3′	
MCP	ISKNV	F: 5′–ATCCCCTCCATCACATCCAGCAAG-3′	AF371960-ORF006
		R: 5′– CATGCAGGCGTTCCAGAAGTCAAG-3′	
GAPDH	TN	F: 5′- CGACAAACTGCCTGGCTCCC -3′	CR734980
		R: 5′- GGGCCGTCCACGGTCTTCT -3′	
GAPDH	ZF	F: 5′- GCCAGCTACGCCAACATCAAG -3′	BC154822
		R: 5′- GTCTCCAACAAAGTCAGAAGAAACGA -3′	
Type I IFN	TN	F: 5′-AATGAGACGGCTGCTCTGTTCG-3′	AJ544904
		R: 5′-AGATTGTCCGCCTGTTGGGTC -3′	
	ZF	F: 5′-AGGTGGAGGACCAGGTGAAGTTTT -3′	NM_207640
		R:5′-TCAGACGATTTTCTGTGCAGTATGTTAA -3′	
Type II IFN (IFN-γ)	TN	F: 5′-AGGGTAACCACGGTGATGGGC -3′	CAF95605[a]
		R: 5′-CGCTGGGATGTAGGAACCTTTGA -3′	
	ZF	F: 5′-ATTCCTGCCTCAAAATGGTGCTAC -3′	AB194272
		R: 5′-AGAATCGGGTTCTCGCTCCTG -3′	
TNF-α	TN	F: 5′-CGGTGAGGTCGGCCGTGTCA -3′	CAF98738[b]
		R: 5′-TTGGTCTCGGTCCACAGTTTGTG -3′	R: 5′-TTGGTCTCGGTCCACAGTTTGTC -3′
	ZF	F: 5′-TCAAAGTCGGGTGTATGGAGGG -3′	AY427649
		R: 5′-CCTGGGTCTTATGGAGCGTGAA -3′	

TN, *Tetraodon nigroviridis*; ZF, zebrafish.
[a] Identified by comparing its encoding product with the IFN-γ protein sequence of zebrafish (GenBank accession no. AB158361) and *Takifugu rubripes* (GenBank accession no. CAE82301; identified by Zou et al., 2004).
[b] Indentified by comparing its encoding product with the TNF-α protein sequence of *T. rubripes* (GenBank accession no. NP_001033074; identified by Savan et al., 2005).

Quantitative real-time PCR

A total of 400 *Tetraodon* and 600 zebrafish were challenged with purified ISKNV in the same way as described in the Fish and virus section.

To determine the quantities of ISKNV GE in the infected tissues, the spleens of 15 *Tetraodon* per sample time were collected at 1, 2, 3, 4, 5, 6, 8, 10, 12, and 14 dpi. As a comparison, spleens of ISKNV-infected zebrafish were sampled at 1, 2, 3, 4, 5, 6, and 8 dpi in the same way. ISKNV in each sample were quantified by quantitative real-time PCR as previously described (Xu et al., 2008). The levels of ISKNV GE per microgram (μg) of tissue DNA were calculated.

For quantitative real-time RT–PCR analysis of levels of gene transcription, *Tetraodon* spleens at 0, 4, 8, 12, and 16 hpi and 1, 2, 3, 4, 5, 6, 8, 10, 12, and 14 dpi were sampled. Each sample was collected from 15 fish. As a comparison, spleens of zebrafish were sampled at 0, 4, 8, 12, and 16 hpi and at 1, 2, 3, 4, 5, 6, and 8 dpi. Each sample was collected from 15 fish. As controls, spleens of healthy *Tetraodon* and zebrafish injected with PBS were sampled in an identical manner to that of the challenged groups. Total RNA of each sample was purified and reverse transcribed to cDNA by reverse transcriptase. Quantitative real-time RT–PCR was performed as previously described (Xu et al., 2008). The genes analyzed and their specific primers are listed in Table 1. Expression levels were normalized to glyceraldehydes phosphate dehydrogenase (GAPDH) gene transcription in both *Tetraodon* and zebrafish. For types I and II interferon genes and TNF-α gene, the expression levels at 0 hpi were defined as basal levels, and the transcription levels in other samples were calculated based on basal transcription levels. For the VP23R and MCP genes of ISKNV, the expression ratio values of samples were calculated over the highest observed values, which were defined as 100%.

Acknowledgments

References

Atrasheuskaya, A., Petzelbauer, P., Fredeking, T.M., Ignatyev, G., 2003. Anti-TNF antibody treatment reduces mortality in experimental dengue virus infection. FEMS Immunol. Med. Microbiol. 35 (1), 33–42.
Bradley, J.R., 2008. TNF-mediated inflammatory disease. J. Pathol. 214 (2), 149–160.
Bui, P., Bagherie-Lachidan, M., Kelly, S.P., 2010. Cortisol differentially alters claudin isoforms in cultured puffer fish gill epithelia. Mol. Cell. Endocrinol. 317 (1–2), 120–126.
Caipang, C.M., Hirono, I., Aoki, T., 2006. Immunogenicity, retention and protective effects of the protein derivatives of formalin-inactivated red seabream iridovirus (RSIV) vaccine in red seabream, *Pagrus major*. Fish Shellfish Immunol. 20 (4), 597–609.
Cawthorn, W.P., Sethi, J.K., 2008. TNF-alpha and adipocyte biology. FEBS Lett. 582 (1), 117–131.
Chen, H.C., Hofman, F.M., Kung, J.T., Lin, Y.D., Wu-Hsieh, B.A., 2007. Both virus and tumor necrosis factor alpha are critical for endothelium damage in a mouse model of dengue virus-induced hemorrhage. J. Virol. 81 (11), 5518–5526.
Chinchar, V.G., Essbauer, S., He, J.G., Hyatt, A., Miyazaki, T., Seligy, V., Williams, T., 2005. Family Iridoviridae. In: Fauquet, C.M., Mayo, M.A., Maniloff, J., Desselberger, U., Ball, L.A. (Eds.), Virus Taxonomy, VIIIth Report of the International Committee on Taxonomy of Viruses. Elsevier/Academic Press, London, pp. 145–162.
Clelland, E.S., Bui, P., Bagherie-Lachidan, M., Kelly, S.P., 2010. Spatial and salinity-induced alterations in claudin-3 isoform mRNA along the gastrointestinal tract of the pufferfish *Tetraodon nigroviridis*. Comp. Biochem. Physiol. A Mol. Integr. Physiol. 155 (2), 154–163.
Darai, G., Anders, K., Koch, H.G., Delius, H., Gelderblom, H., Samalecos, C., Flugel, R.M., 1983. Analysis of the genome of fish lymphocystis disease virus isolated directly from epidermal tumours of *Pleuronectes*. Virology 126 (2), 466–479.
Darai, G., Delius, H., Clarke, J., Apfel, H., Schnitzler, P., Flugel, R.M., 1985. Molecular cloning and physical mapping of the genome of fish lymphocystis disease virus. Virology 146 (2), 292–301.
Dardalhon, V., Korn, T., Kuchroo, V.K., Anderson, A.C., 2008. Role of Th1 and Th17 cells in organ-specific autoimmunity. J. Autoimmun. 31 (3), 252–256.
Delius, H., Darai, G., Flugel, R.M., 1984. DNA analysis of insect iridescent virus 6: evidence for circular permutation and terminal redundancy. J. Virol. 49 (2), 609–614.
Deng, M., He, J.G., Zuo, T., Weng, S.P., Zeng, K., Lu, L., Zhou, S.Y., Long, Q.X., 2000. Infectious spleen and kidney necrosis virus (ISKNV) from *Siniperca chuatsi*: development of a PCR detection method and the new evidence of iridovirus. Chin. J. Virol. 4, 365–369.
Dong, C., Weng, S., Shi, X., Xu, X., Shi, N., He, J., 2008. Development of a mandarin fish *Siniperca chuatsi* fry cell line suitable for the study of infectious spleen and kidney necrosis virus (ISKNV). Virus Res. 135 (2), 273–281.
Go, J., Lancaster, M., Deece, K., Dhungyel, O., Whittington, R., 2006. The molecular epidemiology of iridovirus in Murray cod (*Maccullochella peelii peelii*) and dwarf gourami (*Colisa lalia*) from distant biogeographical regions suggests a link between trade in ornamental fish and emerging iridoviral diseases. Mol. Cell. Probes 20 (3–4), 212–222.
He, J.G., Zeng, K., Weng, S.P., Chan, S.M., 2000. Systemic disease caused by an iridovirus-like agent in cultured mandarin fish, *Siniperca chuatsi* (Basillewsky), in China. J. Fish Dis. 23, 219–222.

He, J.G., Deng, M., Weng, S.P., Li, Z., Zhou, S.Y., Long, Q.X., Wang, X.Z., Chan, S.M., 2001. Complete genome analysis of the mandarin fish infectious spleen and kidney necrosis iridovirus. Virology 291 (1), 126–139.

He, J.G., Zeng, K., Weng, S.P., Chan, S.M., 2002. Experimental transmission, pathogenicity and physical–chemical properties of infectious spleen and kidney necrosis virus (ISKNV). Aquaculture 204, 11–24.

Inouye, K., Yamano, K., Maeno, Y., Nakajima, K., Matsuoka, M., Wada, Y., Sorimachi, M., 1992. Iridovirus infection of cultured red sea bream, Pagrus major. Fish Pathol. 27, 19–27.

Jaillon, O., Aury, J.M., Brunet, F., Petit, J.L., Stange-Thomann, N., Mauceli, E., Bouneau, L., Fischer, C., Ozouf-Costaz, C., Bernot, A., Nicaud, S., Jaffe, D., Fisher, S., Lutfalla, G., Dossat, C., Segurens, B., Dasilva, C., Salanoubat, M., Levy, M., Boudet, N., Castellano, S., Anthouard, V., Jubin, C., Castelli, V., Katinka, M., Vacherie, B., Biemont, C., Skalli, Z., Cattolico, L., Poulain, J., De Berardinis, V., Cruaud, C., Duprat, S., Brottier, P., Coutanceau, J.P., Gouzy, J., Parra, G., Lardier, G., Chapple, C., McKernan, K.J., McEwan, P., Bosak, S., Kellis, M., Volff, J.N., Guigo, R., Zody, M.C., Mesirov, J., Lindblad-Toh, K., Birren, B., Nusbaum, C., Kahn, D., Robinson-Rechavi, M., Laudet, V., Schachter, V., Quetier, F., Saurin, W., Scarpelli, C., Wincker, P., Lander, E.S., Weissenbach, J., Roest Crollius, H., 2004. Genome duplication in the teleost fish Tetraodon nigroviridis reveals the early vertebrate proto-karyotype. Nature 431 (7011), 946–957.

Jeong, J.B., Kim, H.Y., Jun, L.J., Lyu, J.H., Park, N.G., Kim, J.K., Jeong, H.D., 2008. Outbreaks and risks of infectious spleen and kidney necrosis virus disease in freshwater ornamental fishes. Dis. Aquat. Organ. 78 (3), 209–215.

Jung, S.J., Oh, M.J., 2000. Iridovirus-like infection associated with high mortalities of striped beakperch, Oplegnathus fasciatus (Temmink et Schlegel), in southern coastal areas of the Korean peninsula. J. Fish Dis. 23, 223–226.

Katagiri, H., Ito, Y., Ito, S., Murata, T., Yukihiko, S., Narumiya, S., Watanabe, M., Majima, M., 2008. TNF-alpha induces thromboxane receptor signaling-dependent microcirculatory dysfunction in mouse liver. Shock 30 (4), 463–467.

Kudo, H., Takahara, T., Yata, Y., Kawai, K., Zhang, W., Sugiyama, T., 2009. Lipopolysaccharide triggered TNF-alpha-induced hepatocyte apoptosis in a murine non-alcoholic steatohepatitis model. J. Hepatol. 51 (1), 168–175.

Lutfalla, G., Roest Crollius, H., Stange-Thomann, N., Jaillon, O., Mogensen, K., Monneron, D., 2003. Comparative genomic analysis reveals independent expansion of a lineage-specific gene family in vertebrates: the class II cytokine receptors and their ligands in mammals and fish. BMC Genomics 4 (1), 29.

Martina, B.E., Koraka, P., Osterhaus, A.D., 2009. Dengue virus pathogenesis: an integrated view. Clin. Microbiol. Rev. 22 (4), 564–581.

McFadden, G., Mohamed, M.R., Rahman, M.M., Bartee, E., 2009. Cytokine determinants of viral tropism. Nat. Rev. Immunol. 9 (9), 645–655.

Novelli, F., Casanova, J.L., 2004. The role of IL-12, IL-23 and IFN-gamma in immunity to viruses. Cytokine Growth Factor Rev. 15 (5), 367–377.

Roest Crollius, H., Jaillon, O., Bernot, A., Dasilva, C., Bouneau, L., Fischer, C., Fizames, C., Wincker, P., Brottier, P., Quetier, F., Saurin, W., Weissenbach, J., 2000a. Estimate of human gene number provided by genome-wide analysis using Tetraodon nigroviridis DNA sequence. Nat. Genet. 25 (2), 235–238.

Roest Crollius, H., Jaillon, O., Dasilva, C., Ozouf-Costaz, C., Fizames, C., Fischer, C., Bouneau, L., Billault, A., Quetier, F., Saurin, W., Bernot, A., Weissenbach, J., 2000b. Characterization and repeat analysis of the compact genome of the freshwater pufferfish Tetraodon nigroviridis. Genome Res. 10 (7), 939–949.

Rowell, J.F., Griffin, D.E., 2002. Contribution of T cells to mortality in neurovirulent Sindbis virus encephalomyelitis. J. Neuroimmunol. 127 (1–2), 106–114.

Savan, R., Kono, T., Igawa, D., Sakai, M., 2005. A novel tumor necrosis factor (TNF) gene present in tandem with the TNF-alpha gene on the same chromosome in teleosts. Immunogenetics 57 (1–2), 140–150.

Sepulcre, M.P., Alcaraz-Perez, F., Lopez-Munoz, A., Roca, F.J., Meseguer, J., Cayuela, M.L., Mulero, V., 2009. Evolution of lipopolysaccharide (LPS) recognition and signaling: fish TLR4 does not recognize LPS and negatively regulates NF-kappaB activation. J. Immunol. 182 (4), 1836–1845.

Song, K., Mariappan, R., Khosravi-Far, R., 2008. Analysis of TNF-related apoptosis-inducing ligand in vivo through bone marrow transduction and transplantation. Methods Enzymol. 446, 315–331.

Templeton, S.P., Perlman, S., 2008. Role of IFN-gamma responsiveness in CD8 T-cell-mediated viral clearance and demyelination in coronavirus-infected mice. J. Neuroimmunol. 194 (1–2), 18–26.

Tidona, C.A., Darai, G., 1997. The complete DNA sequence of lymphocystis disease virus. Virology 230 (2), 207–216.

Volff, J.N., 2005. Genome evolution and biodiversity in teleost fish. Heredity 94 (3), 280–294.

Volff, J.N., Bouneau, L., Ozouf-Costaz, C., Fischer, C., 2003. Diversity of retrotransposable elements in compact pufferfish genomes. Trends Genet. 19 (12), 674–678.

Wang, Y.Q., Lu, L., Weng, S.P., Huang, J.N., Chan, S.M., He, J.G., 2007. Molecular epidemiology and phylogenetic analysis of a marine fish infectious spleen and kidney necrosis virus-like (ISKNV-like) virus. Arch. Virol. 152 (4), 763–773.

Wilhelm, P., Wiede, F., Meissner, A., Donhauser, N., Bogdan, C., Korner, H., 2005. TNF but not Fas ligand provides protective anti-L. major immunity in C57BL/6 mice. Microbes Infect. 7 (15), 1461–1468.

Williams, T., 1996. The iridoviruses. Adv. Virus Res. 46, 345–412.

Xu, X., Zhang, L., Weng, S., Huang, Z., Lu, J., Lan, D., Zhong, X., Yu, X., Xu, A., He, J., 2008. A zebrafish (Danio rerio) model of infectious spleen and kidney necrosis virus (ISKNV) infection. Virology 376 (1), 1–12.

Zou, J., Yoshiura, Y., Dijkstra, J.M., Sakai, M., Ototake, M., Secombes, C., 2004. Identification of an interferon gamma homologue in Fugu, Takifugu rubripes. Fish Shellfish Immunol. 17 (4), 403–409.